Electronic Supplementary Material (ESI) for Catalysis Science & Technology.

Extending the 2D Covalent Organic Frameworks by Inserting Anthracene for Promoted White-light-mediated Photocatalysis

Yiqiong Liu,[a] Zehao Zhao,[a] Wenshuo Xu,[a] and Weitao Gong*[a]

[a] State Key Laboratory of Fine Chemicals, School of Chemical Engineering, Dalian University of Technology, Dalian 116024, PR China

Corresponding author, E-mail: wtgong@dlut.edu.cn

Contents

Section 1 Characterization

All required solvents and reagents were purchased from commercial sources unless otherwise specified. ^{1}H NMR spectra was obtained by Bruker Avance II 400 instrument. The structure of polymers was mainly characterized by the Fourier transform infrared (FT-IR) spectroscopy, Nuclear magnetic resonance (NMR) spectra, and Powder X-ray diffraction (PXRD). The FT-IR and ^{13}C NMR spectra were recorded from JASCO IR-4100 and Bruker AVANCEIIIHD600 spectrometer, respectively. PXRD pattern was acquired on Bruker D8 Advance with Cu Kα radiation (λ = 1.5418 Å). The Quantachrome Autosorb iQ was used to analyze the porosity. Uv-vis diffuse reflectance spectra were conducted on JASCO V-750 spectrometer. Mettler Toledo TGA/DSC $^{3+}$ thermal analyzer was used to carry out thermogravimetric analysis (TGA). The morphologies were carried out on FEI Nova NanoSEM 450 and JEM2100. Density functional theory (DFT) computational and visualization were performed by BDF software within Device Studio program and Multiwfn program. The CHI 760E electrochemical workstation was employed to examine the photoelectric properties of two COFs, using the Mott-Schottky curve test, EIS Nyquist plots test, and instantaneous photocurrent test in a standard three-electrode system. Detection of reactive oxygen intermediate species were obtained on a Bruker A200-9.5/12 EPR spectrometer. Time-resolved photoluminescence decay profiles were obtained in Edinburgh Instruments FLS1000.

Section 2 Synthetic procedures

Synthesis of 1,3,5-Tris (4-aminophenyl) triazine (TAPT) [1]

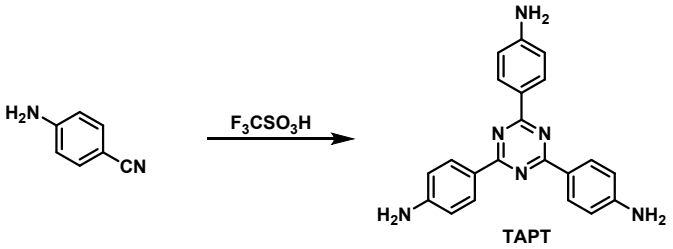

TAPT

Under an inert atmosphere, 4-aminobenzonitrile (0.77 g, 6.54 mmol) and trifluoromethanesulfonic acid (4 mL, 44.4 mmol) were added to a three-neck round-bottom flask at 0 °C. After warming to room temperature, the reaction mixture was stirred continuously for 24 h, and then distilled water (40 mL) was poured into the mixture, followed by 1M NaOH for neutralization. Typically, a deep-orange precipitate appeared with increasing pH value under basic conditions. The precipitate was finally filtered, and washed with water and MeOH to afford a pale-yellow product (0.40 mg, 52%). ^{1}H NMR ($CDCl_3$, 400 MHz) δ (ppm) = 8.36 (d, J = 8.5 Hz, 6H), 6.71 (d, J = 8.5 Hz, 6H), 5.89 (s, 6H).

Synthesis of anthracene-9,10-dicarbaldehyde (AND) [2]

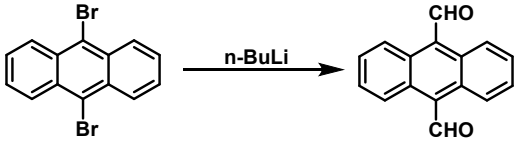

AND

A solution of 9,10-dibromoanthracene (4.77 g, 13 mmol) in anhydrous THF (200 mL) was added to a three-neck round-bottom flask and cooled down to -78°C under an inert atmosphere, then n-butyllithium (16.9 mL, 27 mmol) was added dropwise to the solution and the mixture was stirred at -78°C for an hour. Next, anhydrous DMF (4 mL, 52 mmol) was added to the reaction mixture dropwise, and the mixture was brought to room temperature to stir overnight. Diluted with 15 mL water, the resulting precipitate was filtered, washed, and purified by recrystallization in DMSO to obtain an orange needle-like solid (1.55 g, 51%). ^{1}H NMR ($CDCl_3$, 400 MHz) δ (ppm) = 11.47 (s, 2H), 8.72 (d, 4H), 7.69 (d, 4H).

Synthesis of AND-TAPT

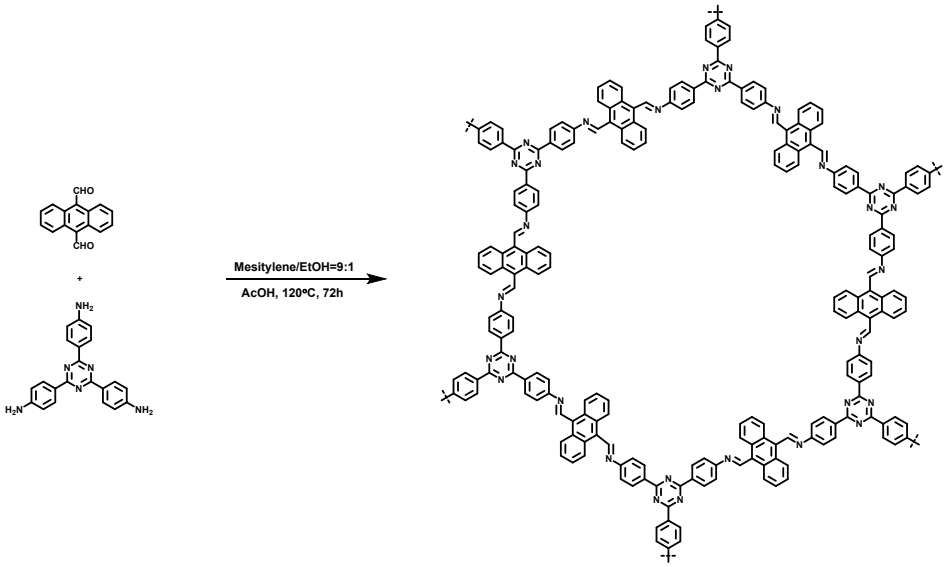

58

59 **Synthesis of PDA-TAPT**

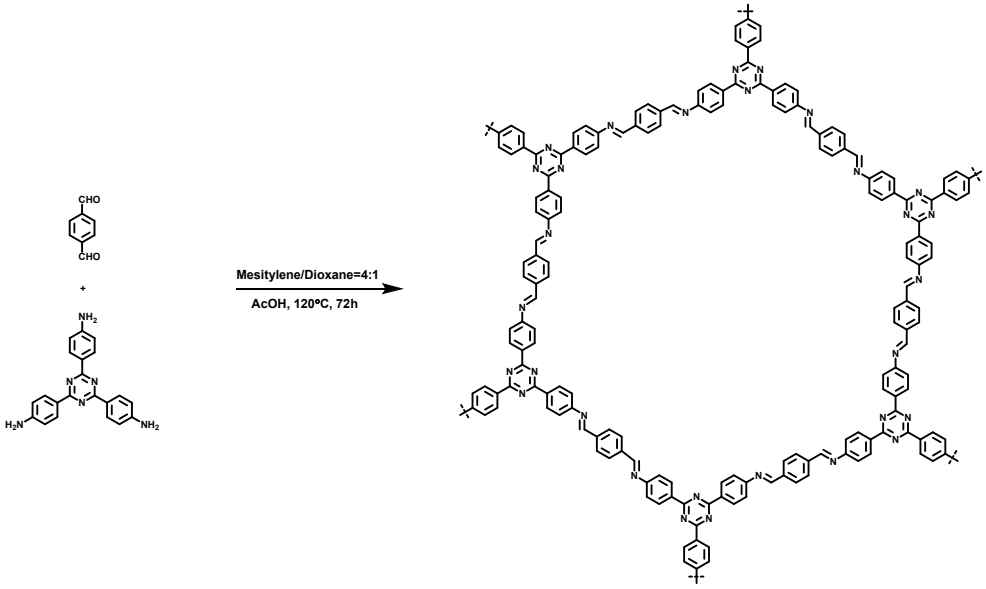

60

61

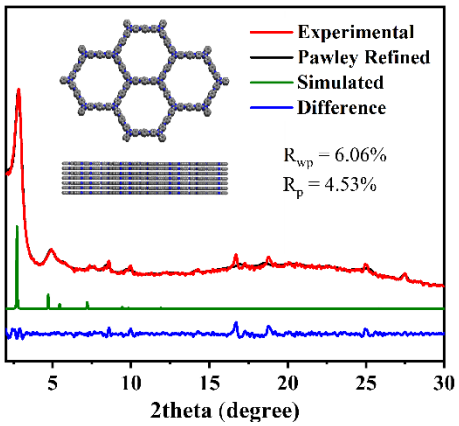

62

63 **Fig. S1** PXRD pattern of PDA-TAPT.

Section 3 ^{13}C Nuclear Magnetic Resonance (NMR) spectra

The ^{13}C cross-polarization magic angle spinning (CP/MAS) NMR spectrum of AND-TAPT further confirmed the presence of imine bond with C=N resonance at 163 ppm. The strong signals at 125 and 129 ppm can be assigned to the carbon atoms of the phenyl groups, while the relatively weaker signal at~194 ppm corresponds to the carbon atoms of terminal aldehyde groups in the AND-TAPT network. More importantly, the peak at 174 ppm further corroborated the successful incorporation of triazine into the network. Those clearly showed that the condensation reaction was completed confirming completion of the reaction.

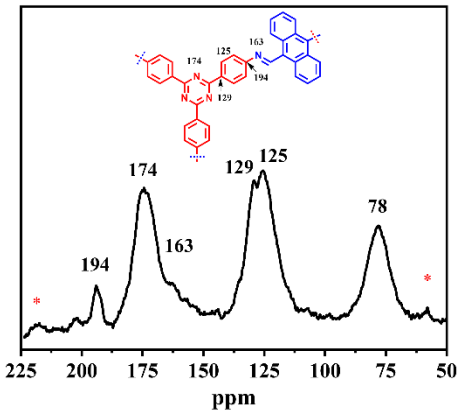

Fig. S2 Solid state ^{13}C NMR spectra of AND-TAPT.

Section 4 HOMO and LUMO values

After being optimized by the BDF software with ωB97XD/6-31G (d, p), the orbital energy of the selected monomer structure was calculated [3, 4]. Then, the HOMO and LUMO orbital diagrams were shown by using the Multiwfn program [5]. As shown in Table S1, both two amine-aldehyde pairs could form effective D-A pairs.

Table S1 Simulation of HOMO and LUMO values (eV) of monomers and COFs.

	TAPT	PDA	AND	PDA-TAPT	AND-TAPT
HOMO (eV)	-5.356	-7.271	-5.919	-9.236	-8.368
LUMO (eV)	-1.107	-2.661	-3.054	-0.679	-0.988
Band gap (eV)	4.249	4.610	2.865	8.557	7.381

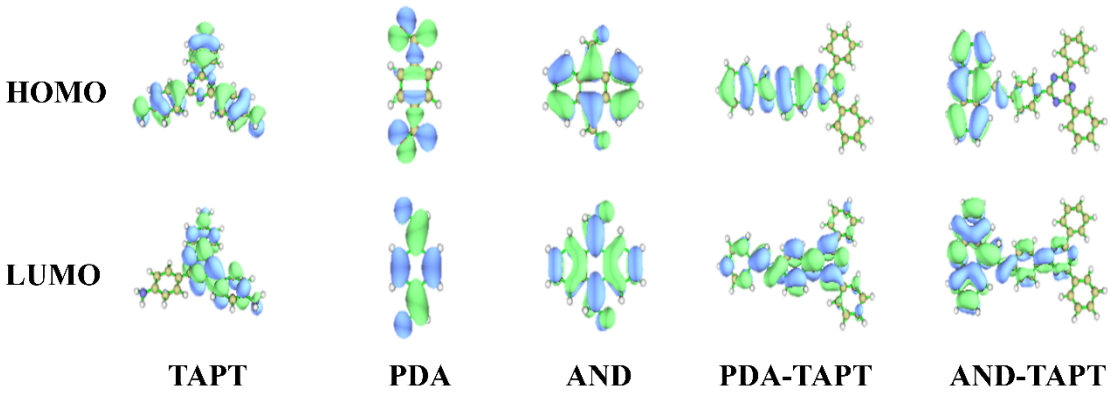

Fig. S3 Simulation of HOMO and LUMO of monomers and COFs.

Section 5 Exciton binding energy (E_b)

After being optimized by the BDF software with ωB97XD/6-31G (d, p), the IP, EA, and E_{opt} were calculated by using the BDF software with M06-2X/6-31G (d, p), and then exciton binding energy (E_b) was obtained by subtracting E_{opt} from E_{fund} [4, 6].

Table S2 Calculated exciton binding energy.

	IP (eV)	EA (eV)	E_{fund} (eV)	E_{opt} (eV)	E_b (eV)
AND-TAPT	7.215	0.838	6.377	3.411	2.966
PDA-TAPT	7.927	0.584	7.343	3.994	3.349

IP: ionization potential;

EA: electron affinity;

E_{fund}: fundamental gap, $E_{fund} = IP - EA$;

E_{opt}: optical gap, the energy gap between S_0 and S_1;

E_b: exciton binding energy, $E_b = E_{fund} - E_{opt}$.

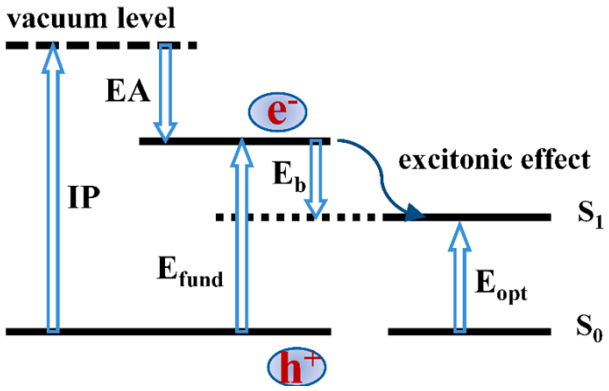

Fig. S4 Schematic of various energy gaps.

Section 6. Detection of reactive oxygen species (ROS)

EPR measurements of TEMP-$^1O_2$: 2 mg photocatalyst was added to 0.1 M TEMP (3 ml in CH_3CN), and the mixture was continuously irradiated for 2 h with a white lamp (10 W LED) before measurement.

UV-vis measurements of N, N, N', N'-tetramethyl-p-phenylenediamine (NTPD): Typically, two standard solutions of NTPD were prepared separately in acetonitrile. 2 mg photocatalyst was added to one of the solutions and both the solutions were stirred for 2 h under constant irradiation by visible white lamp (10 W LED). Observe the absorption band in the 450-650 nm range.

Section 7 Photoelectrochemical measurements

The CHI 760E electrochemical workstation and a standard three-electrode system were used to analyze the optical and electronic properties of COFs. A 0.1 M Na_2SO_4 solution, platinum wire electrode, and Ag/AgCl electrode were used as the electrolyte, counter electrode, and reference electrode, respectively. 3 mg of photocatalyst and 50 μL 5wt% Nafion were mixed in 1 mL of EtOH and sonicated for 30 min. For photocurrent measurement, the mixture was homogeneously dispersed onto FTO (size: 10×20 mm^2; coated area: 10×10 mm^2) to obtain the working electrode, and the switch of the irradiation from 300 W Xe lamp irradiation was realized by a cardboard covered with tinfoil. For Mott-Schottky analysis and EIS measurement, the mixture was dropped onto glass carbon to obtain the working electrode.

Section 8 Photocatalytic experiment supplement

Table S3 Heterogeneous photocatalysts for oxidative coupling of benzylamine.

Photocatalyst	Light	Conditions	t (h)	Conv. (%)	Reference
Py-BSZ COF (5 mg)	520 nm LED (15 W)	benzylamine (0.2 mmol), CH_3CN (2 mL), rt, air	12	99	[7]
COF-TpPa (10 mg)	420 nm LED (5 W)	benzylamine (0.9 mmol), CH_3CN (6 mL), rt, O_2	8	99	[8]
BDTA-TAPT (6 mg)	Xe lamp (λ=420-780 nm, 300 W)	benzylamine (0.1 mmol), CH_3CN (3 mL), rt, O_2	3	97	[9]
AN-POP (0.5 mmol%)	460nm LED (24 W)	benzylamine (0.5 mmol), CH_3CN (5 mL), rt, air	24	99	[10]
TFB-33-DMTH（10 mg）	454nm LED (30 W)	benzylamine (0.2 mmol), H_2O (2 mL), rt, air	20	99	[11]
TFA-TTA-COF (5 mg)	454 nm LED (30 W)	benzylamine (0.2 mmol), H_2O (3 mL), rt, O_2	20	99	[12]
AC-COF (4 mg)	440nm LED (32 W)	benzylamine (0.2 mmol), CH_3CN (2 mL), rt, air	24	99	[13]
PDA-TAPT (1 mmol%, 2 mg)	white LED (10 W)	benzylamine (0.2 mmol), CH_3CN (5 mL), rt, air	24	16	This work
AND-TAPT (1 mmol%, 3 mg)	white LED (10 W)	benzylamine (0.2 mmol), CH_3CN (5 mL), rt, air	24	99	This work

Table S4 Heterogeneous photocatalysts for selective oxidation of thioanisole.

Photocatalyst	Light	Conditions	t (h)	Conv. (%)	Reference
TCPP-CMP (10 mg)	white LED (100 W)	thioanisole (0.5 mmol), CH_3CN/H_2O (10 mL, 1:1), rt, O_2	16	99	[14]
HP-1 (10 mg)	540 nm LED (10 W)	thioanisole (0.2 mmol), CH_3CN / CH_3OH (4 mL, 3:1), rt, O_2	8	99	[15]
COF-NUST-31 (4 mg)	460 nm LED (30 W)	thioanisole (0.1 mmol), CH_3CN (1.5 mL), rt, O_2	4	99	[16]
$NQ\text{-}COF_{TfppyPh}$ (5 mg)	460nm LED (18 W)	thioanisole (1 mmol), CH_3OH (1.5 mL), rt, air	12	99	[17]
TPDH-PTBA（5mg）	450nm LED (30 W)	thioanisole (0.15 mmol), CH_3OH (2 mL), rt, O_2	12	99	[18]
Q-COF-T (2 mg)	Xe lamp (300 W)	thioanisole (0.1 mmol), CH_3CN (5 mL), rt, O_2	3	99	[19]
PDA-TAPT (1 mmol%, 2 mg)	white LED (10 W)	thioanisole (0.2 mmol), EtOH (2 mL), rt, air	15	57	This work
AND-TAPT (1 mmol%, 3 mg)	white LED (10 W)	thioanisole (0.2 mmol), EtOH (2 mL), rt, air	15	99	This work

Fig. S5. The photocatalytic reactions were performed by a photoreactor from WATTCAS WP-TEC-1020HS

Section 9 ^{1}H-NMR results of the reactions

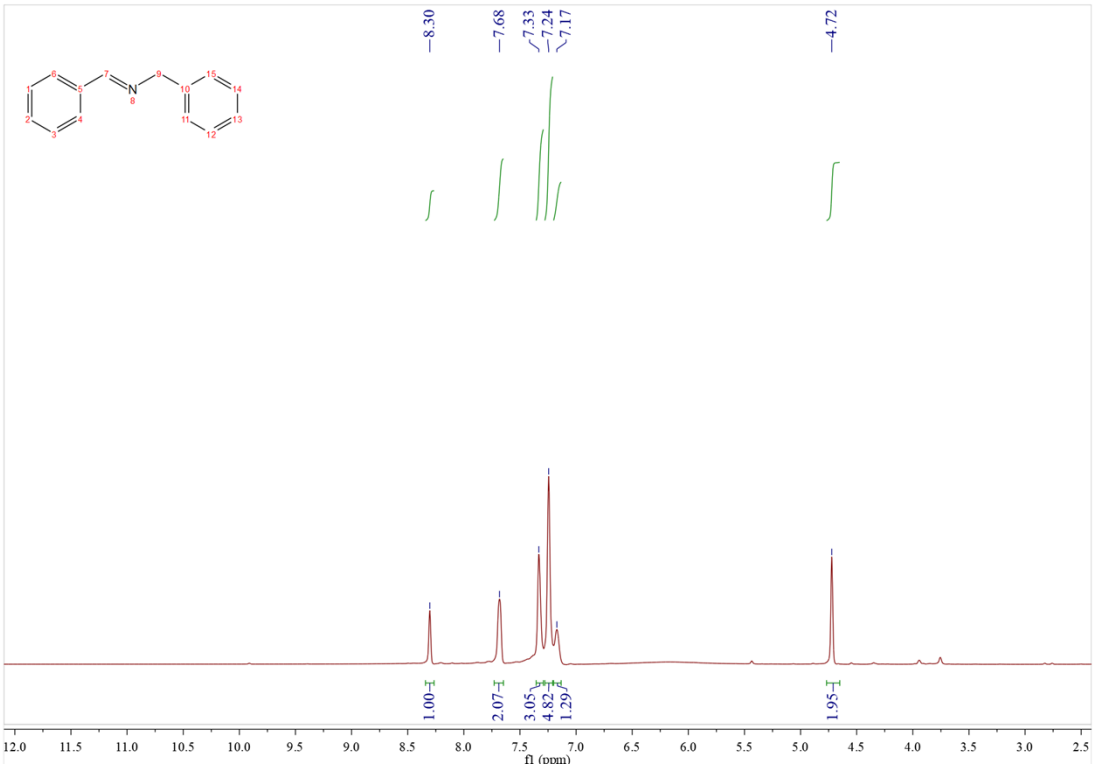

121

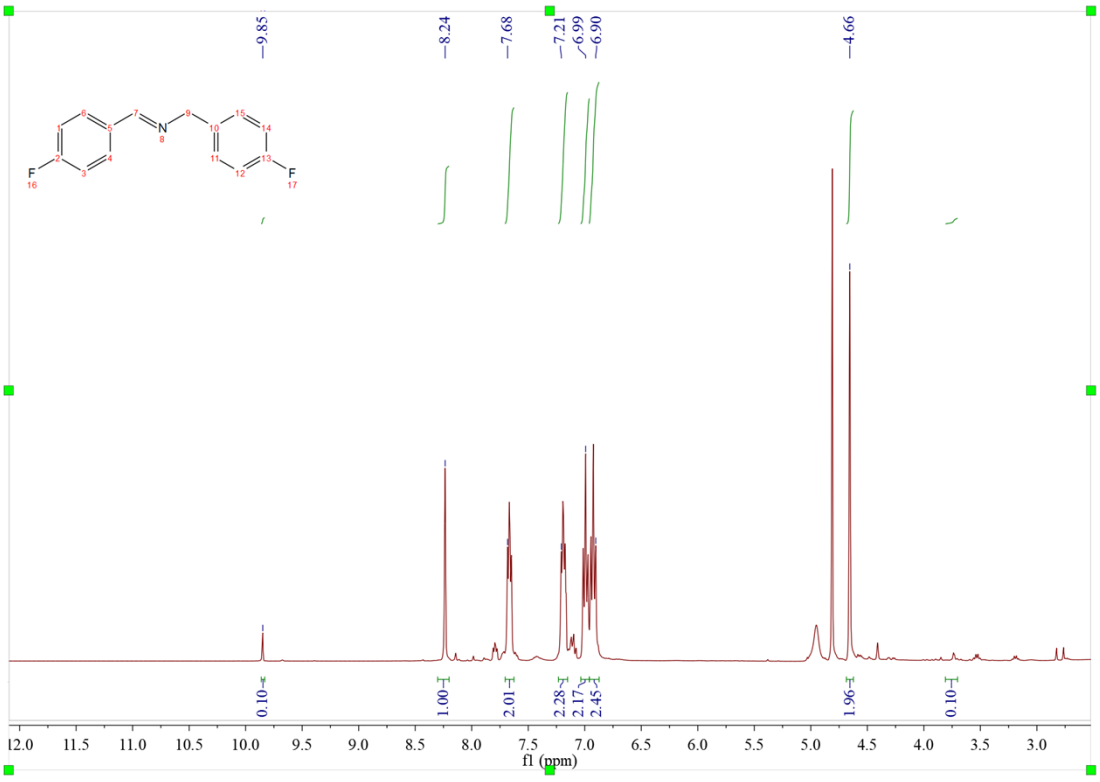

122

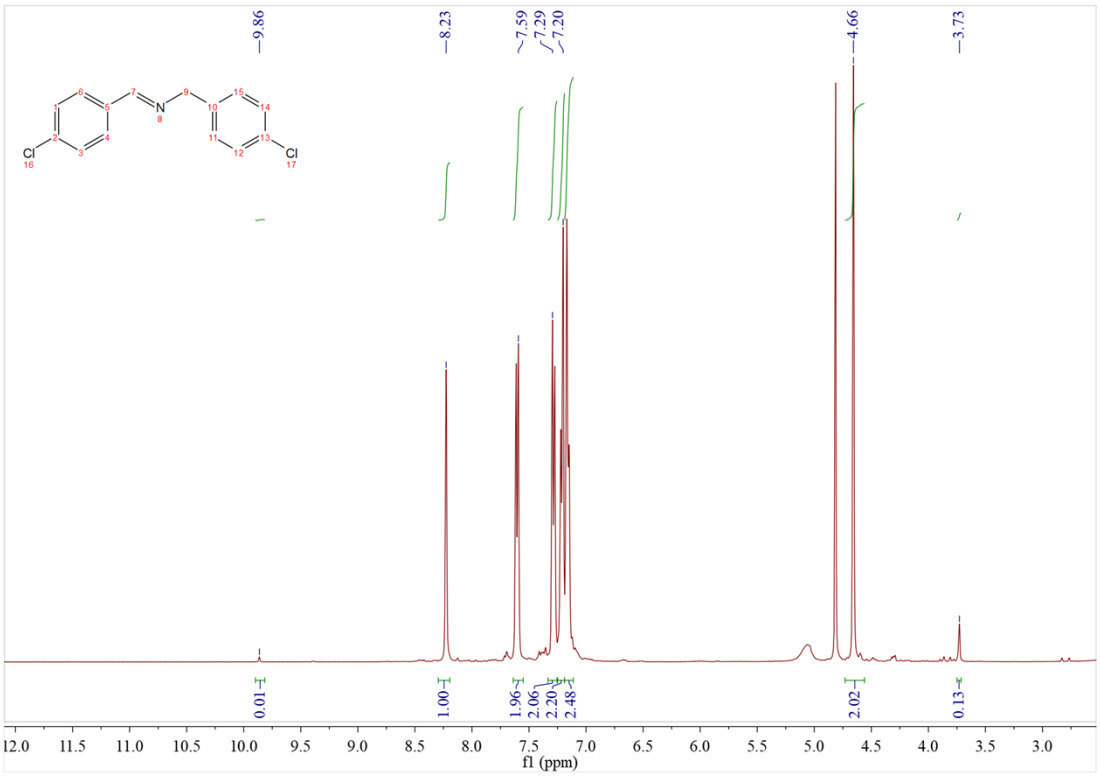
9.86
8.23
7.59
7.29
7.20
4.66
3.73
0.01
1.00
1.96
2.06
2.20
2.48
2.02
0.13
f1 (ppm)

123

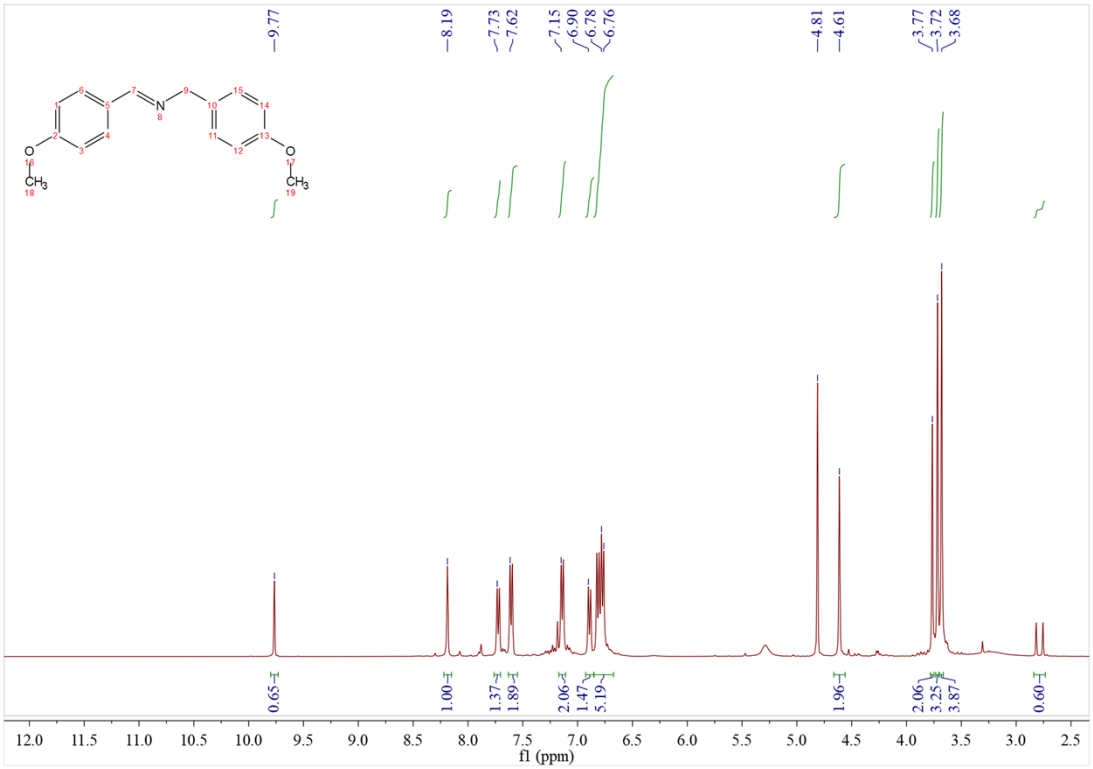
9.77
8.19
7.73
7.62
7.15
6.90
6.78
6.76
4.81
4.61
3.77
3.72
3.68
0.65
1.00
1.37
1.89
2.06
1.47
5.19
1.96
2.06
3.25
3.87
0.60
f1 (ppm)

124

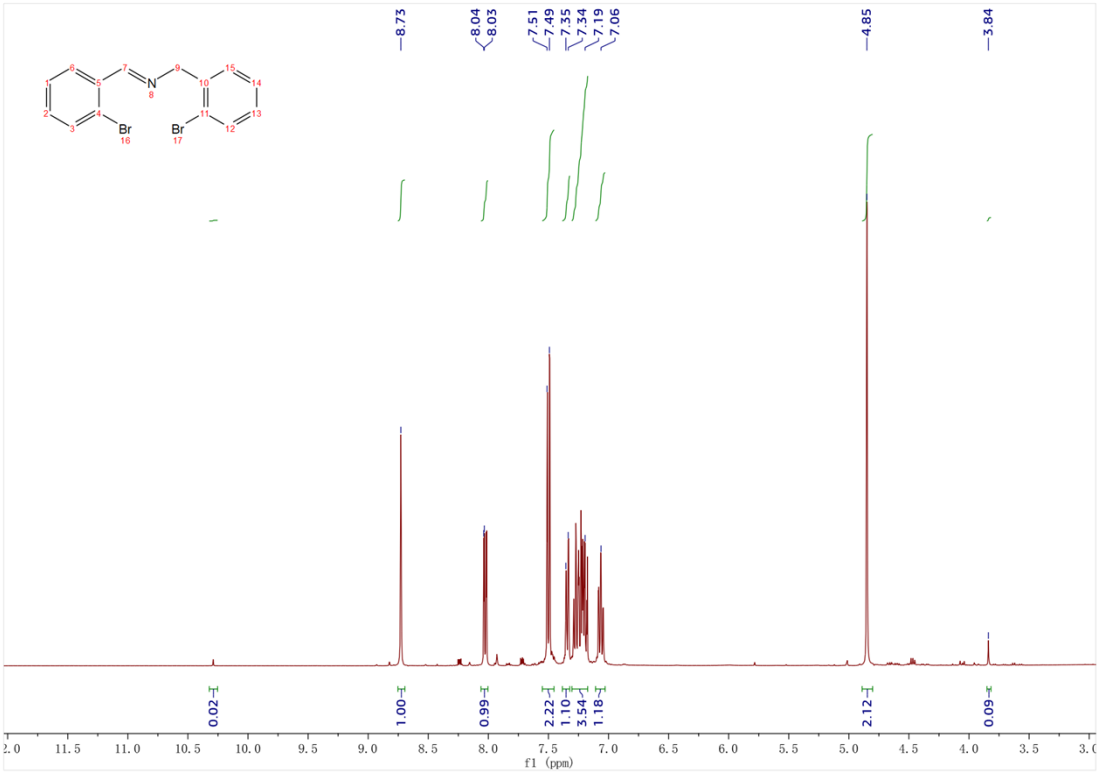
8.73
8.04
8.03
7.51
7.49
7.35
7.34
7.19
7.06
4.85
3.84
Br
Br
0.02
1.00
0.99
2.22
1.10
3.54
1.18
2.12
0.09
f1 (ppm)

125

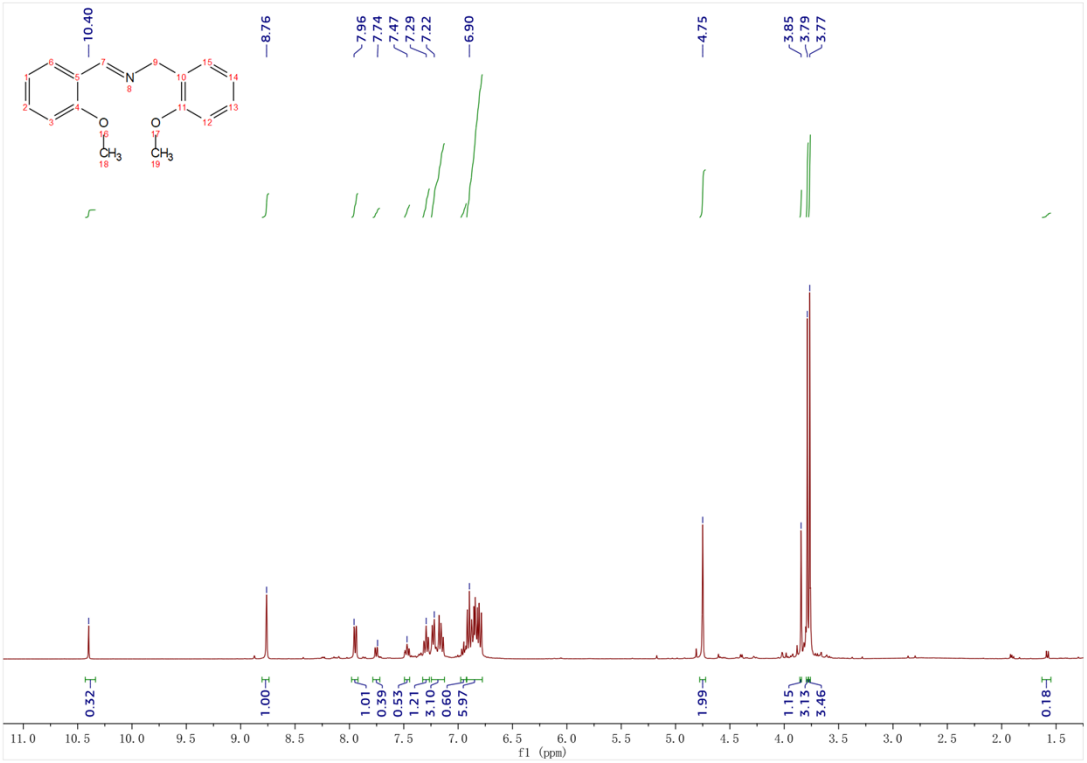
10.40
8.76
7.96
7.74
7.47
7.29
7.22
6.90
4.75
3.85
3.79
3.77
O
CH3
O
CH3
0.32
1.00
1.01
0.39
0.53
1.21
3.10
0.60
5.97
1.99
1.15
3.13
3.46
0.18
f1 (ppm)

126

127

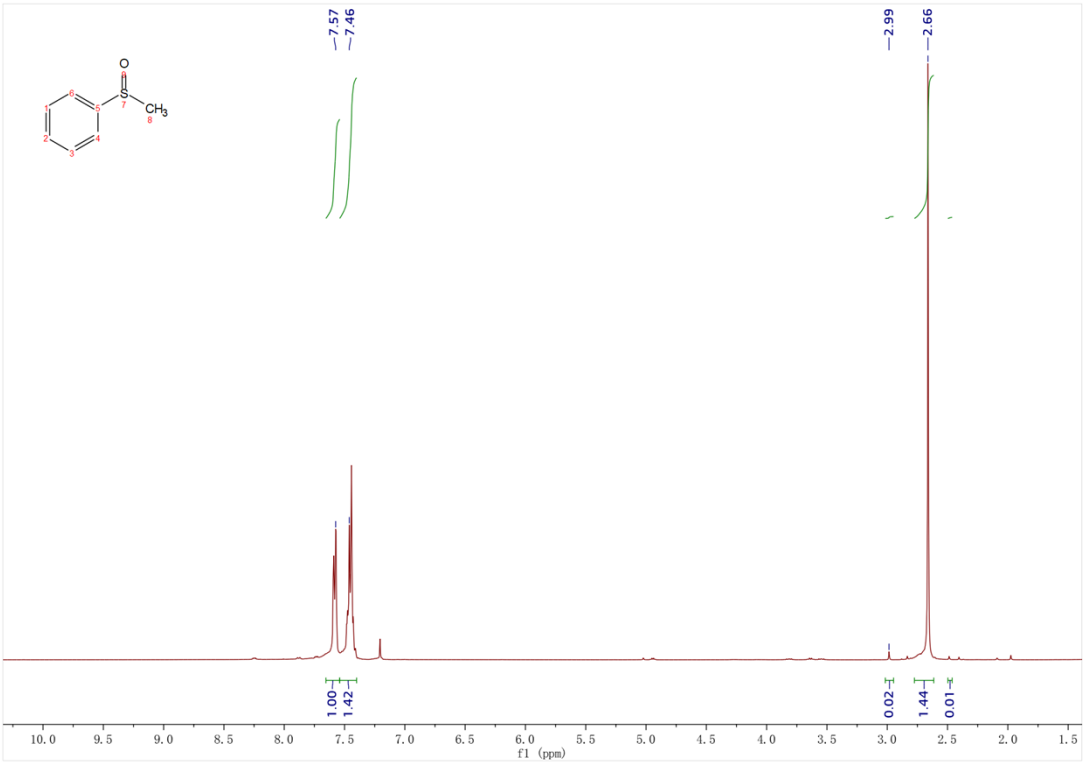
7.57
7.46
2.99
2.66
1.00
1.42
0.02
1.44
0.01
f1 (ppm)

128

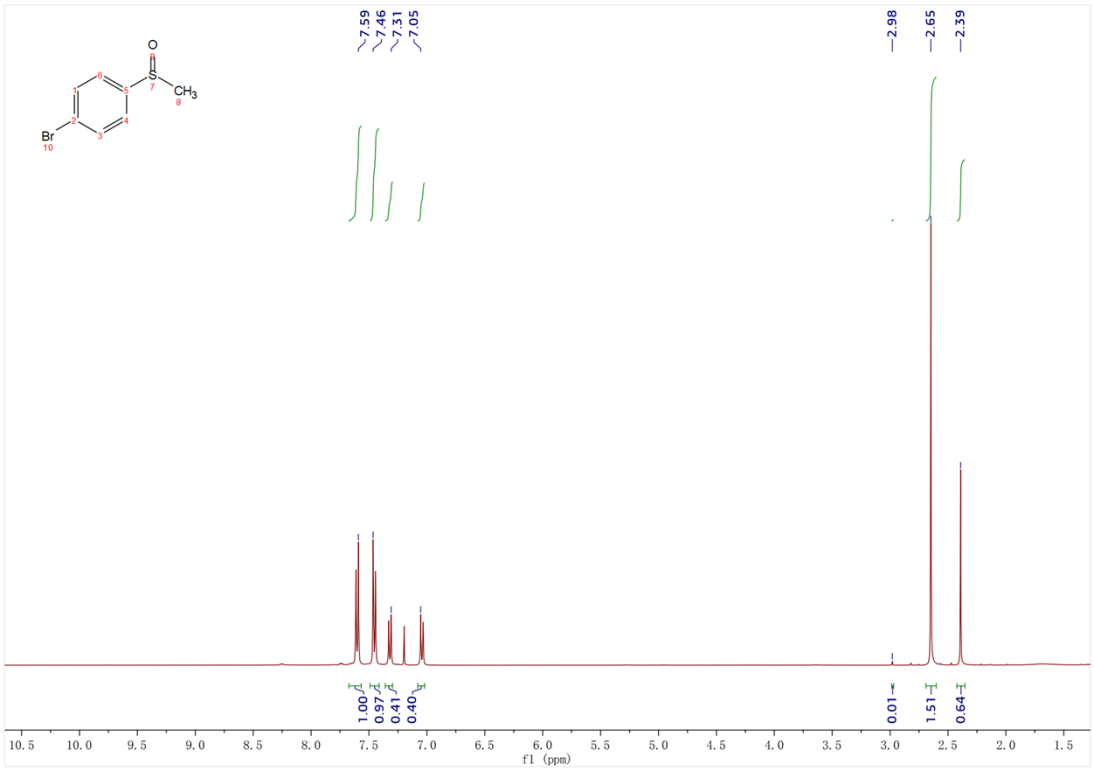
7.59
7.46
7.31
7.05
2.98
2.65
2.39
1.00
0.97
0.41
0.40
0.01
1.51
0.64
f1 (ppm)

129

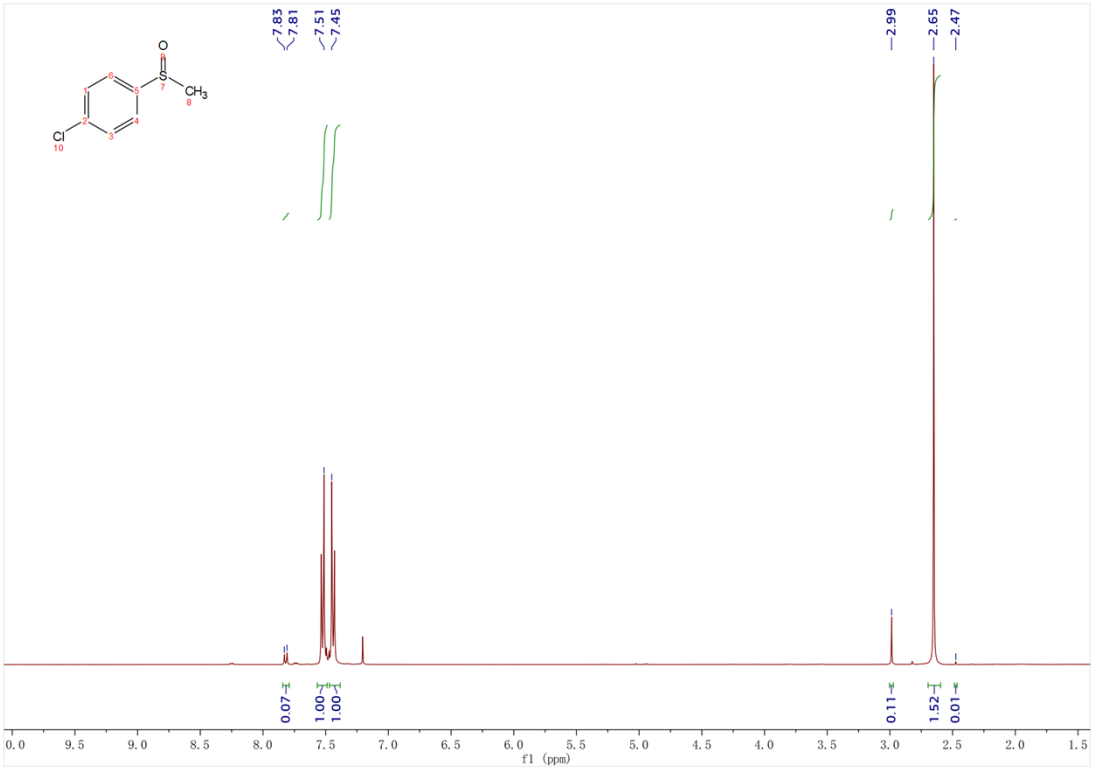
7.83
7.81
7.51
7.45
2.99
2.65
2.47
0.07
1.00
1.00
0.11
1.52
0.01
f1 (ppm)

130

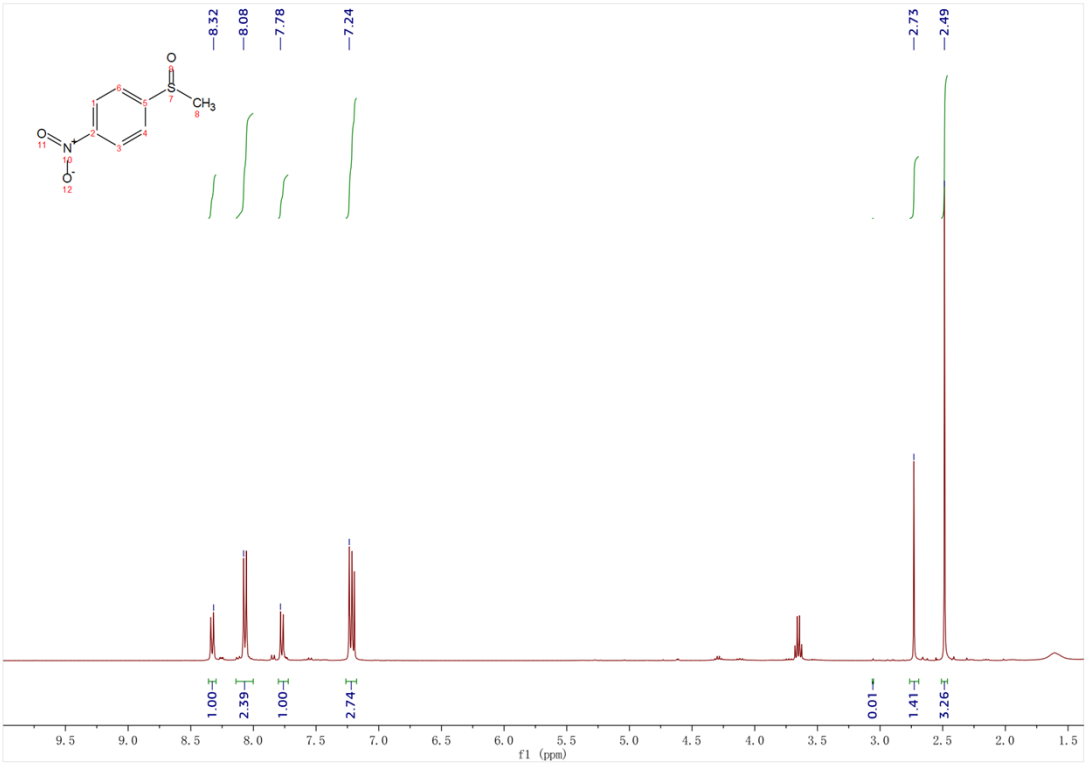
8.32
8.08
7.78
7.24
2.73
2.49
1.00
2.39
1.00
2.74
0.01
1.41
3.26
f1 (ppm)

131

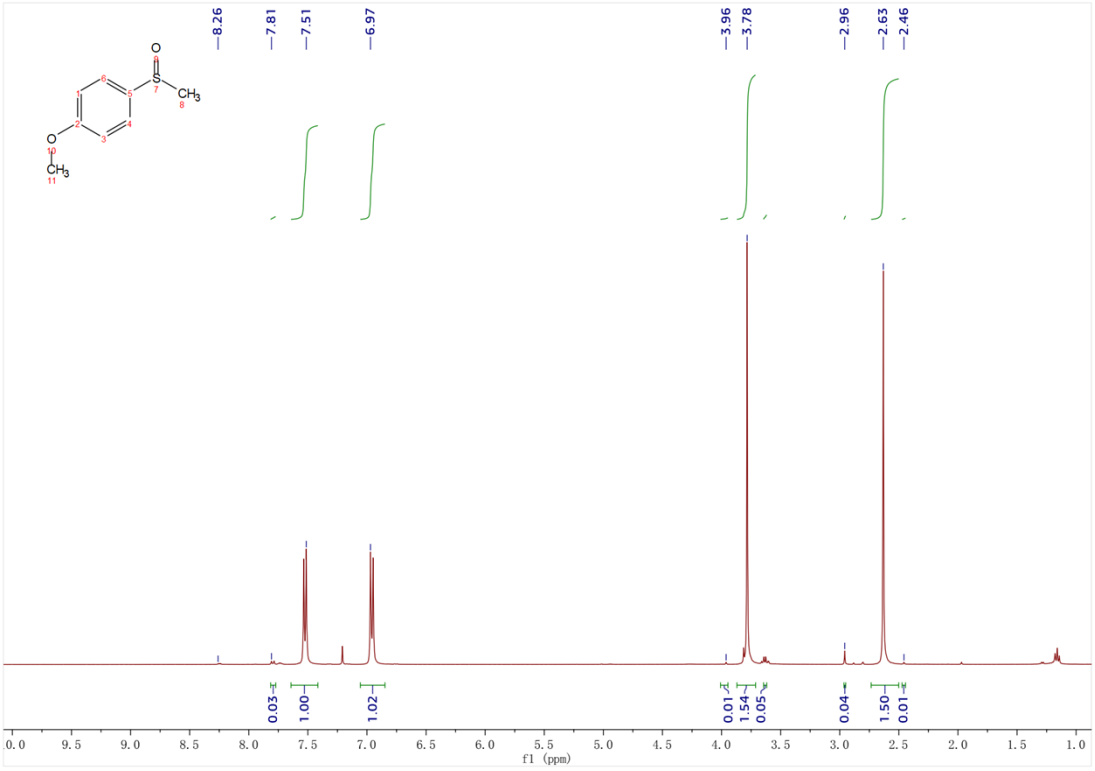
8.26
7.81
7.51
6.97
3.96
3.78
2.96
2.63
2.46
0.03
1.00
1.02
0.01
1.54
0.05
0.04
1.50
0.01
f1 (ppm)

132

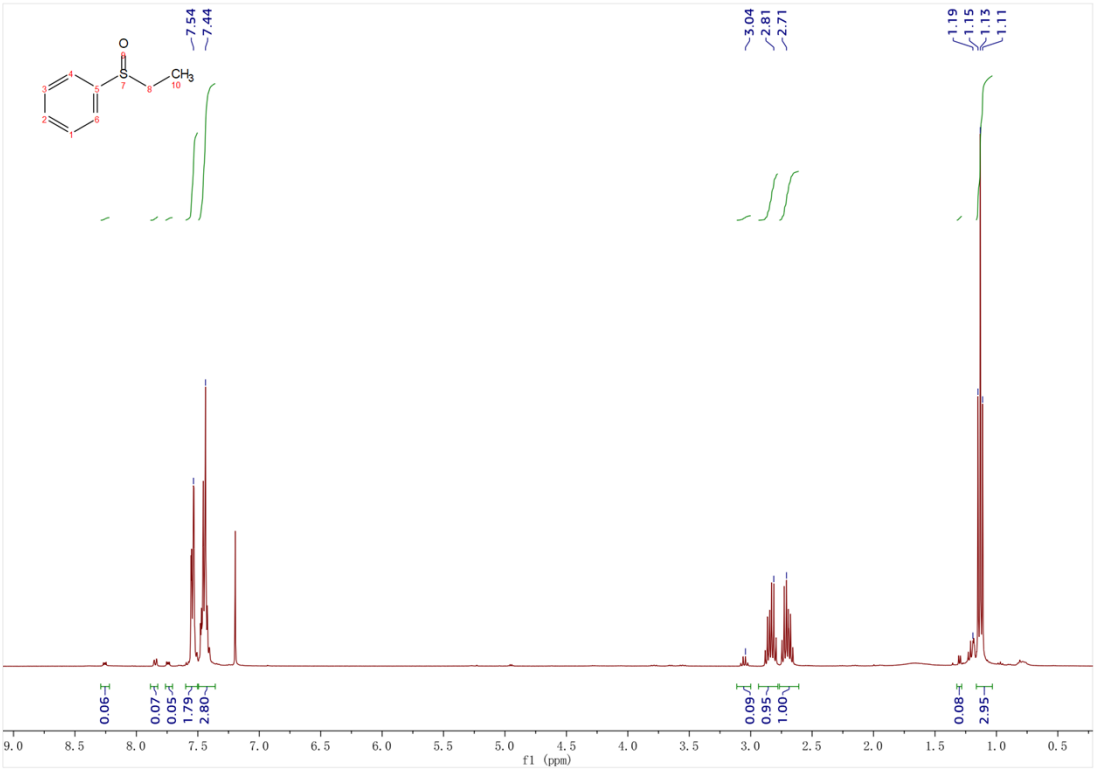
7.54
7.44
3.04
2.81
2.71
1.19
1.15
1.13
1.11
0.06
0.07
0.05
1.79
2.80
0.09
0.95
1.00
0.08
2.95
f1 (ppm)

133

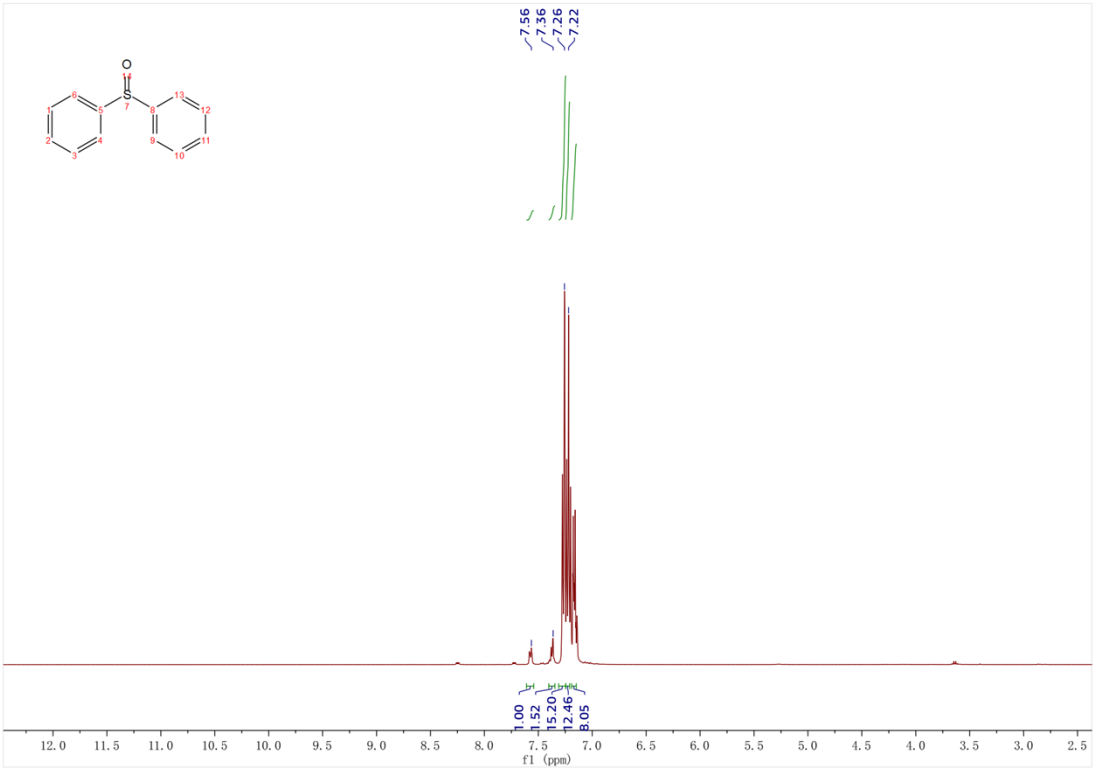
7.56
7.36
7.26
7.22
1.00
1.52
15.20
12.46
8.05
12.0 11.5 11.0 10.5 10.0 9.5 9.0 8.5 8.0 7.5 7.0 6.5 6.0 5.5 5.0 4.5 4.0 3.5 3.0 2.5
f1 (ppm)

134

135

Section 10 References

1. Z. Li, J.-a. Wang, S. Ma, Z. Zhang, Y. Zhi, F. Zhang, H. Xia, G. Henkelman and X. Liu, *Appl. Catal., B*, 2022, **310**, 121335.
2. A. E. Lee, M. R. Grace, A. G. Meyer and K. L. Tuck, *Tetrahedron Lett.*, 2010, **51**, 1161-1165.
3. Y. Zhang, B. Suo, Z. Wang, N. Zhang, Z. Li, Y. Lei, W. Zou, J. Gao, D. Peng, Z. Pu, Y. Xiao, Q. Sun, F. Wang, Y. Ma, X. Wang, Y. Guo and W. Liu, *J. Chem. Phys.*, 2020, **152**.
4. Z. Wang, Z. Li, Y. Zhang and W. Liu, *J. Chem. Phys.*, 2020, **153**.
5. T. Lu and F. Chen, *J. Comput. Chem.*, 2012, **33**, 580-592.
6. Y. Qian, Y. Han, X. Zhang, G. Yang, G. Zhang and H.-L. Jiang, *Nat. Commun.*, 2023, **14**, 3083.
7. S. Li, L. Li, Y. Li, L. Dai, C. Liu, Y. Liu, J. Li, J. Lv, P. Li and B. Wang, *ACS Catal.*, 2020, **10**, 8717-8726.
8. Z. Wu, X. Huang, X. Li, G. Hai, B. Li and G. Wang, *Sci. China Chem.*, 2021, **64**, 2169-2179.
9. Q. Li, J. Wang, Y. Zhang, L. Ricardez-Sandoval, G. Bai and X. Lan, *ACS Appl. Mater. Interfaces*, 2021, **13**, 39291-39303.
10. L. Liu, W.-D. Qu, K.-X. Dong, Y. Qi, W.-T. Gong, G.-L. Ning and J.-N. Cui, *Chem. Commun.*, 2021, **57**, 3339-3342.
11. S. Liu, Q. Su, W. Qi, K. Luo, X. Sun, H. Ren and Q. Wu, *Catal. Sci. Technol.*, 2022, **12**, 2837-2845.
12. W. Qi, Q. Wu, W. Wang, J. Feng and Q. Su, *J. Photochem. Photobiol. A: Chem.*, 2023, **437**, 114502.
13. Q. Lin, Y. Yusran, J. Xing, Y. Li, J. Zhang, T. Su, L. Yang, J. Suo, L. Zhang, Q. Li, H. Wang, Q. Fang, Z.-T. Li and D.-W. Zhang, *ACS Appl. Mater. Interfaces*, 2024, **16**, 5869-5880.
14. J. Jiang, Z. Liang, X. Xiong, X. Zhou and H. Ji, *ChemCatChem*, 2020, **12**, 3523-3529.
15. T.-Y. Qiu, Y.-N. Zhao, W.-S. Tang, H.-Q. Tan, H.-Y. Sun, Z.-H. Kang, X. Zhao and Y.-G. Li, *ACS Catal.*, 2022, **12**, 12398-12408.
16. Z. Gu, J. Wang, Z. Shan, M. Wu, T. Liu, L. Song, G. Wang, X. Ju, J. Su and G. Zhang, *J. Mater. Chem. A*, 2022, **10**, 17624-17632.
17. X. Zhao, H. Pang, D. Huang, G. Liu, J. Hu and Y. Xiang, *Angew. Chem. Int. Ed.*, 2022, **61**, e202208833.
18. Y. Hu, Y. Ji, Z. Qiao and L. Tong, *Microporous Mesoporous Mater.*, 2023, **362**, 112767.
19. R. Xue, Y.-S. Liu, H. Guo, W. Yang and G.-Y. Yang, *J. Colloid Interface Sci.*, 2024, **655**, 709-716.